Zwitterionic-silane copolymer for ultra stable and bright biomolecular probes based on fluorescent quantum dot nanoclusters.

Fatimata Dembele, Mariana Tasso, Laura Trapiella-Alfonso, Xiang Zhen Xu, Mohamed Hanafi, Nicolas Lequeux, Thomas Pons

Zwitterionic-silane copolymer for ultra stable and bright biomolecular probes based on fluorescent quantum dot nanoclusters.

*Fatimata DEMBELE[1], Mariana TASSO[2], Laura TRAPIELLA-ALFONSO[1†], Xiangzhen XU[1], Mohamed HANAFI[3], Nicolas LEQUEUX[1] and Thomas PONS[1]**

[1] Laboratoire de Physique et d'Etude des Matériaux, ESPCI Paris, PSL Research University, CNRS UMR8213, Université Pierre et Marie Curie, Sorbonne-Universités, 10 rue Vauquelin, 75005 Paris, France

[2] Soft Matter Laboratory, INIFTA-CONICET, calle 64 y diagonal 113, 1906 La Plata, Argentina

[3] Laboratoire Sciences et Ingénierie de la Matière Molle, ESPCI Paris, PSL Research University, CNRS UMR 7615, Université Pierre et Marie Curie, Sorbonne-Universités, 10 rue Vauquelin, 75005 Paris, France

KEYWORDS. Zwitterionic Copolymers, Biodetection, Quantum Dots, Nanoclusters, Silica

ABSTRACT. Fluorescent semiconductor quantum dots (QDs) exhibit several unique properties that make them suitable candidates for biomolecular sensing, including high brightness, photostability, broad excitation and narrow emission spectra. Assembling these QDs into robust and functionalizable nanosized clusters (QD-NSCs) can provide fluorescent probes that are several orders of magnitude brighter than individual QDs, thus allowing an even greater sensitivity of detection with simplified instrumentation. However, the formation of compact, anti-fouling, functionalizable and stable QD-NSCs remains a challenging task, especially for a use at ultra-low concentrations for single-molecule detection. Here, we describe the development of fluorescent QD-NSCs envisioned as a tool for fast and sensitive biomolecular recognition. Firstly, QDs were assembled into very compact 100-150 nm diameter spherical aggregates; the final QD-NSCs were obtained by growing a cross-linked silica shell around these aggregates. Hydrolytic stability in several concentration and pH conditions is a key requirement for a potential and efficient single-molecule detection tool. However, hydrolysis of Si–O–Si bonds leads to desorption of monosilane-based surface groups at very low silica concentrations or in a slightly basic medium. Thus, we designed a novel multidentate copolymer, composed of multiple silane as well as zwitterionic monomers. Coating silica beads with this multidentate copolymer provided a robust surface chemistry that was demonstrated to be stable against hydrolysis, even at low concentrations. Copolymer-coated silica beads also showed low-fouling properties and high colloidal stability in saline solutions. Furthermore, incorporation of additional azido-monomers enabled easy functionalization of QD-NSCs using copper-free bio-orthogonal cyclooctyne-azide click chemistry, as demonstrated by a biotin-streptavidin affinity test.

1. INTRODUCTION

With the ever increasing demand for cheaper, faster and more sensitive bioassays, colloidal light-emitting semi-conductor nanocrystals (quantum dots or QDs) have emerged as ideal candidates for biomolecular probe design. As compared to organic dyes, QDs are resistant to photobleaching and very bright : they can be used to achieve a highly sensitive detection.[1–10] They also present narrow, composition- and size-dependent emission spectra, as well as a large absorption cross section that allows simultaneous excitation of several QD populations at a single wavelength; these unique properties have regularly been exploited for multiplexed detection.[4–6]

Such inorganic particles are routinely synthesized in organic apolar solvents because this synthetic route enables a better control over their size, shape and composition.[11] As a consequence, they are initially capped with hydrophobic ligands and their transfer into aqueous solutions for biological applications requires a modification of their surface chemistry. Several strategies have been developed to solubilize inorganic nanoparticles in water, including encapsulation in amphiphilic copolymers,[2,7,12–15] growth of a silica shell,[1,5,8,16–26] or ligand exchange, which consists in replacing the initial hydrophobic ligands with hydrophilic ones.[9,11,26,27] The resulting water-soluble nanocrystals can be used in a wide variety of applications, including immunohistochemistry, FRET sensing, cell labelling and single protein tracking.[1–7,10,15]

Recently, well-defined and colloidally stable spherical nanosized clusters (NSCs), obtained by assembling tens to thousands of individual nanoparticles, have attracted increasing interest.[12,20,28] QD-NSCs, in particular, exhibit remarkable photostability and superior brightness that can be detected at the single particle level with higher efficiencies and simplified optical setups as

compared to their individual QD counterparts, while also maintaining the unique QD spectral properties. QD-NSCs stand out as valuable tools for multiplexed detection of trace levels of biomarkers, down the single molecule level without requiring signal amplification.[2,3,8,29]

The simplest strategy to assemble hydrophobic nanoparticles such as QDs into hydrophilic and spherical colloidal nanosized aggregates is the well-established emulsification-evaporation technique.[20,30,31] Briefly, emulsions of volatile organic solvent containing the nanoparticles are formed in water and stabilized by surfactants; the organic solvent is then evaporated, which yields dry assemblies of the initial nanoparticles. Notably, the choice of surfactant has a critical impact on the morphology and stability of the resulting clusters. It was demonstrated that protocols that involve small molecular surfactants lead to the formation of compact and size-controlled clusters.[20,31] However, these small surfactants are labile and remain in a dynamic equilibrium of adsorption and desorption at the hydrophobic/hydrophilic interface. As a consequence, they tend to quickly desorb from the surface after dilution and washing steps, thus making them unsuitable for QD-NSCs functionalization. In contrast, longer amphiphilic copolymers remain strongly bound to the interface but reproducible well-controlled cluster shapes are difficult to obtain[2,12] and hydrophobic polymer patches may remain exposed to the aqueous medium. Additionally, both types of coating may allow individual or small QDs clusters to leak from the NSCs with time.[23]

Considering all these reasons, we chose to grow a silica shell around each QD cluster. Not only does this cross-linked, gel-like shell prevent QD leakage from the QD-NSCs core, but it also enables a rather easy surface tailoring of NSCs.[1,5,8,16–23,25,32] Surface functionalization of silica particles is well documented using alkoxysilanes, and this strategy works well in concentrated solutions. However since the NSCs that we obtained are envisioned as single molecule detection

probes, our surface chemistry should also be stable under highly dilute conditions. Silica particles are particularly affected by hydrolysis of Si-O-Si bonds at highly-diluted concentrations. For example, Diedrich et al. reported hydrolysis rates of 10^{-7}-10^{-8} mol.g^{-1}. s^{-1} for silica beads at neutral pH.[33] This, under infinite dilution conditions, corresponds to the loss of a monolayer equivalent on a 200 nm bead in only a few hours. Hydrolysis might be accelerated under various circumstances,[34–36] eg. in more basic medium, or in the presence of residual amino-silanes. While concentrated silica solutions remain stable due to favorable hydrolysis/condensation equilibrium, we demonstrate herein that the dissolution occurring in dilute conditions may lead to a rapid loss of surface silane moieties. To circumvent this limitation, we designed a novel copolymer composed of multiple anchoring silane groups to increase the stability of NSCs,[37] zwitterionic motifs for aqueous solubility and low-fouling effect, [38–41] as well as reactive groups for further functionalization. When grafted on the surface of Stöber silica beads,[42] the resulting polymer shows greater surface stability than monosilane ligands, provides excellent colloidal stability and limits nonspecific protein adsorption. Moreover, its functionalizable moiety enables efficient QD-NSCs bioconjugation using bio-orthogonal cyclooctyne-azide click chemistry.[43] With these silica-embedded QD-NSC surface-modified by a novel copolymer, we finally demonstrate efficient biodection by binding streptavidin to the particles, as a first model system. [44]

2. MATERIALS AND METHODS

2.1. Chemicals. Acetic acid (CH_3COOH, 99%, Aldrich), ammonium hydroxide (NH_4OH, 28-30%, Aldrich), (3-aminopropyl) triethoxysilane (APTES, $C_9H_{23}NO_3Si$, ≥98%, Sigma-Aldrich),

2,2-azobis(2-amidinopropane) hydrochloride (V50, 97%, $[=NC(CH_3)_2C(=NH)NH_2]_2 \cdot 2HCl$, Aldrich), biotin-agarose (Sigma), bovine serum albumin (BSA, Sigma Aldrich), cetyltrimethylammonium bromide (CTAB, $C_{19}H_{42}BrN$, 99%, Sigma-Aldrich), chloroform ($CHCl_3$,VWR), deuterium oxide (D_2O, 99.9 atom % D, Sigma-Aldrich), dibenzocyclooctyne-Cy3 dye (Cy3-DBCO, $C_{62}H_{84}N_6O_{11}S_3$, Aldrich), dibenzocyclooctyne-N-hydroxysuccinimidyl ester (DBCO-NHS, $C_{23}H_{18}N_2O_5$, Aldrich), dimethyl sulfoxide (DMSO, C_2H_6SO, 99.8%, Sigma-Aldrich), ethanol absolute anhydrous (95%, C_2H_6O, Carlo Erba), HEPES sodium salt ($C_8H_{17}N_2NaO_4S$, 99%, Sigma), hexane (C_6H_{14}, VWR), hydrochloric acid (HCl, Sigma Aldrich), Igepal CO-520 ($(C_2H_4O)_n \cdot C_{15}H_{24}O$, n~5, Sigma), 2-methacryloyloxyethyl phosphorylcholine (PC, $C_{11}H_{22}NO_6P$, Sigma-Aldrich), methanol (95%, CH_3OH, Carlo Erba), methanol-d4 99.8 atom % D (CD_3OD, Sigma-Aldrich), rhodamine B isothiocyanate (RITC, $C_{29}H_{30}ClN_3O_3S$, Sigma-Aldrich), sodium acetate ($C_2H_3NaO_2$, Sigma-Aldrich), sodium bicarbonate ($NaHCO_3$, Sigma Aldrich), sodium carbonate (Na_2CO_3, Prolabo), sodium chloride (NaCl, Sigma-Aldrich), sodium hydroxide (NaOH, 97%, Prolabo), sodium tetraborate ($Na_2B_4O_7$, 99%, Sigma-Aldrich), streptavidin (STA, Biospa) and tetraethyl orthosilicate, 98% (TEOS, $C_8H_{20}O_4Si$, 99%, Sigma) were all used as-received.

2.2. Silica beads preparation and characterization. Silica beads were prepared according to a modified Stöber method[42] described in Supporting Information. The product was precipitated multiple times in ethanol at 5000 g and resuspended in 10 mL ethanol.

Their size distribution was assessed by transmission electron microscopy (TEM) and dynamic light scattering (DLS). TEM images were taken with a JEOL 2010F. Samples were prepared by spreading a drop on an ultra-thin 300 mesh Formvar/carbon-coated copper grid (Agar Scientific),

which was degassed overnight. DLS measurements were carried out on a CGS-3 goniometer system equipped with a HeNe laser (633 nm) and an ALV/LSE-5003 correlator. All samples were initially transferred in a 10 mM HEPES, 150 mM NaCl, pH 7.4 buffer or 10 mM acetate, pH 4.5 buffer or 50 mM bicarbonate, pH 9.5 buffer by 3 rounds of centrifugation (6000 g, 5 min). Data was collected by monitoring the light intensity at different scattering angles between 30 and 150°. The hydrodynamic size distribution was obtained using the CONTIN algorithm as an intensity-averaged hydrodynamic radius.

The zeta potential of silica beads was determined with a Zetasizer Nano ZS90 instrument (Malvern Instruments Ltd.). An estimated 0.1 m^2 of silica beads was transferred into each of the 3 buffers used for DLS measurements and the samples were diluted about 1000 times. 3 series of 50 runs were performed in order to complete the measurements with the Zetasizer software.

2.3. Fluorescent QD-NSCs preparation. CdSe/CdS/ZnS QDs were synthesized as described in the Supporting Information. QD clusters were formed following an emulsion/evaporation protocol. First, 2 nmol of CdSe/CdS/ZnS QDs in hexane were precipitated with ethanol and centrifuged (14,000 g, 10 min). The supernatant was then removed and the QDs were redispersed in 200 µL of chloroform. 750 µL of a 4 mM CTAB aqueous solution was added under vigorous vortexing; the resulting mix was extruded by means of a 1 mL syringe through a 0.80x120mm Sterican needle (Braun) until it became pale-orange and foamy. The mixture was then heated up to 100°C for 10 minutes in order to evaporate the chloroform and to form stable QDs micelles. Afterwards, 10 mL of Igepal CO-520 in pure water (200 $mg.L^{-1}$) were added to the suspension; the mix was left to stir for 5 minutes and centrifuged (5000 g, 4 minutes). This procedure was repeated twice in order to enhance the surfactant exchange ratio on the surface of the clusters.

The clusters were then redispersed in 5 mL ethanol and coated with a silica shell according to a Stöber-modified method.[42] After addition of pure water (1.5 mL), the pH of the suspension was raised with 160 µL of a 28% NH_4OH solution. Finally, 50 µL of triethoxysilane (TEOS) was added and the solution was stirred overnight at room temperature. The resulting QD-NSCs were precipitated multiple times in ethanol (6000 g, 5 min) and finally resuspended in 5 mL of ethanol before being characterized by TEM. QD-NSCs were imaged by TEM as explained for the silica beads.

A photoluminescence spectrum of QD-NSCs was measured with an Edinburgh Instrument spectrometer using a 400 nm excitation wavelength. Fluorescence microscopy was used to compare the fluorescence signal of individual QD-NSCs to that of single QDs from the same synthesis batch. After a set of dilutions, images of individualized single QDs or QD-NSCs deposited onto a coverslip were acquired with a wide-field epifluorescence microscope (IX71 Olympus) using a 60 × 1.2 NA (numerical aperture) water objective, a Chroma filter (λ_{exc}= 450/25 and λ_{em}=610±20), and an electron-multiplying charge coupled device (EM CCD) camera (cascade 512B Roper). The fluorescence signal of individual QD-NSCs relative to single QDs was evaluated using Image-J Software (NIH).

2.4. Synthesis and characterization of P(PC-PTMSi) and P(PC-PTMSi-N_3) copolymers. 2-methacryloyloxyethyl phosphorylcholine (PC, 1.5 g, 5 mmol, 1 equiv.) and 3-(trimethoxysilyl)propyl methacrylate (PTMSi, 134 µL, 1 mmol, 0.2 equiv.) monomers were mixed in methanol (30 mL) with 2,2-azobis(2-amidinopropane) hydrochloride (V50, 9.15 mg, 0.014 mmol, 0.015 equiv.) initiator. The mixture was degassed by argon bubbling for 1 hour at

room temperature before being stirred overnight at 70°C under argon atmosphere, resulting in a limpid colorless P(PC-PTMSi) solution.

The synthesis of P(PC-PTMSi-N_3) was identical to the one described above, only with the addition of *N*-(11-azido-3,6,9-trioxaundecan)methacrylamide (-N_3, 152 mg, 0.5 mmol, 0.1 equiv.) to the initial PC, PTMSi mixture in methanol. The resulting P(PC-PTMSi-N_3) solution was limpid and pale yellow. The protocol that describes the synthesis of *N*-(11-azido-3,6,9-trioxaundecan)methacrylamide is provided in Supporting Information.

P(PC-PTMSi) and P(PC-PTMSi-N_3) were characterized by gel permeation chromatography (GPC, Viscotek GPC MAX, Viscotek VE 2001 GPC Solvent/Sample Module and TDA 302 triple detector array) in 0.5 M $NaNO_3$ aqueous solution. ^{1}H NMR spectroscopy was performed on a 400 MHz Bruker NMR spectrometer at 298 K. FT-IR spectra were performed on a Bruker vertex 70 equipped with an ATR. Purification of the polymer from remaining monomers was performed either using dialysis in methanol (3000 MW cutoff), drying under vacuum and resuspension in CD_3OD or by 3 rounds of ultrafiltration (14000 g, 10 min) with D_2O in vivaspin 500, MW cutoff 10 kDa).

2.5. Polymer-capped silica beads preparation. An estimated of 1 m^2 surface equivalent silica beads were transferred into 100 µL methanol and reacted for 2 hours at 60°C with 400 µL of P(PC-PTMSi) or P(PC-PTMSi-N_3) solutions in methanol, corresponding to about 40 mg polymer. The products, P(PC-PTMSi)- and P(PC-PTMSi-N_3)-coated silica beads, were precipitated multiple times in methanol. P(PC-PTMSi)-coated silica beads in methanol were characterized by thermogravimetric analysis (TGA, SDT Q-600 modulus, TA Instruments).

Their colloidal stability was assessed by Dynamic Light Scattering (DLS) and their zeta potential was determined with a Malvern Zetasizer as described above for silica beads.

2.5.1 Low-fouling properties. The nonspecific adsorption of proteins was tested on P(PC-PTMSi)-coated silica beads as compared to bare silica beads and silica beads coated with a model zwitterionic monosilane, the 3(dimethyl-(3-(trimethoxysilyl)propyl)ammonio)propane-1-sulfonate (SBS). SBS and SBS-coated silica beads were prepared according to the protocol described by Estephan et al. [45]

The test was conducted as follows: rhodamine isothiocyanate (RITC)-labeled bovine serum albumin (BSA) was prepared by adding 40 µL of 5 $mg.mL^{-1}$ RITC in DMSO to 400 µL of a 0.1 M Borate, pH 8 buffer solution containing 4 mg BSA. After being reacted with the dye at 4°C overnight, the labeled proteins were purified by NAP-10 exclusion chromatography (GE Healthcare Life Sciences) and two rounds of ultrafiltration (14000 g, 10 min) in vivaspin 500, MW cutoff 30 kDa). The BSA-RITC proteins were finally resuspended in 10 mM HEPES, 150 mM NaCl, pH 7 buffer and their concentration was estimated using absorption measurements at 280 nm. An estimated 0.1 m^2 bare silica, SBS-coated silica beads or P(PC-PTMSi)-coated silica beads were diluted in 100 µL of HEPES/NaCl buffer, mixed with 100 µL BSA-RITC (25 µM) and agitated for 30 minutes at room temperature. The beads were then purified by 3 cycles of centrifugation at 10,000 g for 10 minutes and resuspension in HEPES/NaCl buffer. The beads were finally resuspended in a 2:1 DMSO: HEPES/NaCl buffer mixture for refractive index matching and their absorbance at 555 nm was measured to quantify the amount of adsorbed BSA-RITC.

2.5.2 Polymer surface stability. The stability of the multidentate polymer P(PC-PTMSi-N_3) versus APTES-derived organosilanes, was assessed on the silica beads' surface for two different pH and concentration conditions.

P(PC-PTMSi-Cy3)-coated beads were prepared as follows. For each condition, an estimated 0.5 m^2 of P(PC-PTMSi-N_3)-coated silica beads in methanol was reacted with dibenzocyclooctyne-Cy3 dye (Cy3-DBCO, 2 nmol). The subsequently obtained P(PC-PTMSi-Cy3)-coated silica beads were washed multiple times by centrifugation (6000 g, 5 min) in methanol before being resuspended in two different buffers and at two different concentrations: (i) 10 mM HEPES, 150 mM NaCl, pH 7.4 buffer at a 0.025 $m^2.mL^{-1}$ concentration, (ii) 10 mM HEPES, 150 mM NaCl, pH 7.4 buffer at a 0.20 $m^2.mL^{-1}$ concentration and (iii) 0.1 M borate, pH 8 buffer at a 0.20 $m^2.mL^{-1}$ concentration.

The stability of these polymer-coated beads was compared to silica beads reacted with fluorescein-labeled APTES (f-APTES). f-APTES was obtained after mixing 0.5 mmol of fluorescein-N-hydroxysuccinimidyl ester (fluorescein-NHS) prepared according to Giovanelli et al.[9] with 0.5 mmol of APTES; the reaction was carried out overnight, in the dark and at room temperature. The product was used without further purification. For each condition, an estimated 0.5 m^2 of silica beads in methanol was reacted with 5 µmol of f-APTES for 2 hours at 60°C. The subsequently obtained f-APTES-modified silica beads were washed multiple times by centrifugation (6000 g, 5 min) in methanol and resupended in the same buffers and at the same concentrations as described for the P(PC-PTMSi-Cy3)-coated silica beads.

P(PC-PTMSi-Cy3) and f-APTES-modified silica beads were stored at room temperature in the dark for 6 days. Polymer and monosilane grafting stability onto the silica surface was determined by following the absorbance of the pellet in search for evidence of surface-released polymer.

Independent samples were considered at each time point. For each absorbance measurement, DMSO was added to each sample in order to obtain a 2:1 DMSO: HEPES/NaCl buffer mixture for refractive index matching. After a centrifugation step (6000 g, 5 min) and sample resuspension in 500 µL, the absorbance at 494 nm (fluorescein) and at 570 nm (Cy3) was measured for the pellet with a UV-vis spectrometer (Shimadzu UV-1800).

2.6. Polymer-capped QD-NSCs. 1 mL of QD-NSCs were coated with P(PC-PTMSi) or P(PC-PTMSi-N_3) according to the same protocol as for the silica beads.

2.6.1 Bioconjugation on polymer-capped QD-NSCs. Dibenzocyclooctyne-functionalized streptavidin (STA-DBCO) was prepared by mixing a streptavidin solution (10 $mg.mL^{-1}$ in 0.1 M Borate buffer, pH 8) with DBCO-NHS (10 $mg.mL^{-1}$ in anhydrous DMSO) at a 1:3 molar ratio. In a typical reaction, 130 nmol of STA were mixed with 390 nmol of DBCO in ~ 800 µL of Borate buffer. The reaction was carried out for 1 hour at room temperature and under agitation. Afterwards, STA-DBCO was purified by three rounds of filtration (14000 g, 10 min) in vivaspin 500, MW cutoff 10 kDa (buffer = 10 mM HEPES, 150 mM NaCl, pH 7.4) and resuspended in 200 µL of the said buffer. 1 m^2 of P(PC-PTMSi-N_3)-coated QD-NSCs was subsequently reacted overnight by copper-free click-chemistry[43] with 100 µL of STA-DBCO in HEPES/NaCl . The two controls to this experiment consisted, on the one hand, in 1 m^2 of P(PC-PTMSi)-coated QD-NSCs, which was also mixed with STA-DBCO following the same procedure and, on the other hand, in 1 m^2 of P(PC-PTMSi-N_3)-coated QD-NSCs mixed with STA without a dibenzocyclooctyne moieity at the same molar ratio.

To demonstrate the effective binding of STA-DBCO to the azide-bearing P(PC-PTMSi-N_3)-coated QD-NSCs and its negligible binding to the negative control, the STA-modified sample

and the controls were exposed to biotin-modified agarose beads. For that, 50 µL of commercial biotin agarose beads were washed in a 10 mM HEPES, 150 mM NaCl, pH 7.4 buffer and were left to react with the three batches of NSCs for 10 min at room temperature. After two washing rounds in the 7.4 buffer, images of the agarose beads deposited onto a coverslip were acquired with a wide-field epifluorescence microscope as described for QD-NSCs.

3. RESULTS AND DISCUSSION

3.1. Fluorescent QD-NSCs preparation. We first synthesized two types of particles. A modified Stöber protocol was used in order to synthesize silica beads with a mean diameter of 172 ± 1 nm as measured by TEM (Supporting Information, Figure S1).

The second type of particles was composed of CdSe/CdS/ZnS core/multishell QD clusters surrounded by an outer silica shell. As depicted in Scheme 1, QD clusters were formed by the emulsion-evaporation method from a QD solution in chloroform and an aqueous solution of CTAB. Compared to other usual surfactants such as the anionic SDS or nonionic Igepal, CTAB surfactants were found to provide clusters with compact spherical shapes and monomodal cluster size distribution. [20,31] Attempts to grow silica directly on these clusters resulted in rapid aggregation, which we believe is due to electrostatic interactions between negatively charged silica oligomers and positively charged clusters' surfaces. CTAB was thus replaced by a nonionic PEGylated surfactant, Igepal CO-520, by a simple and rapid dynamic surfactant exchange. A Stöber-like protocol could then be used to grow a silica shell on the QD clusters, thanks to the

colloidal stability of the PEG-coated clusters and the favorable interactions between the PEG layer and silica.

Scheme 1. Preparation of QD-NSC coated with a silica shell and P(PC-PTMSi-N_3) copolymer.

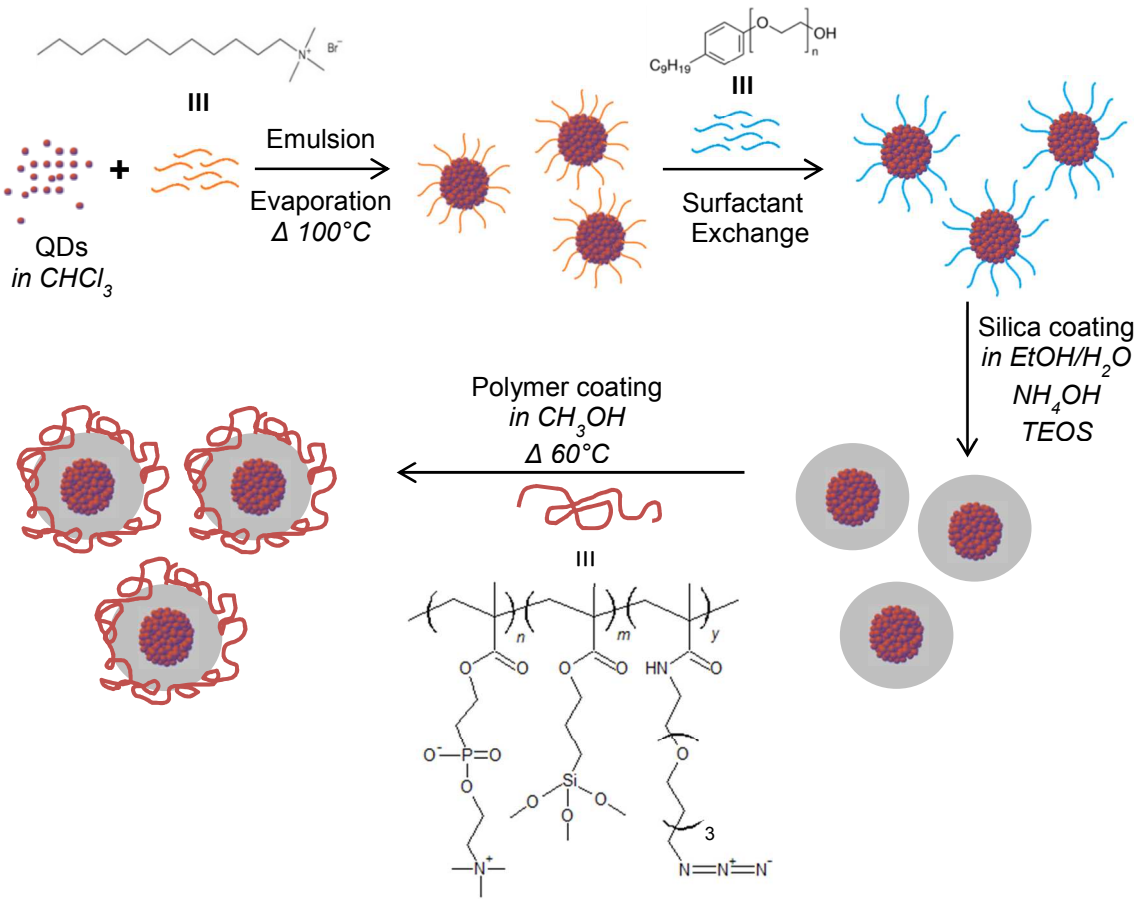

The conditions described in the experimental section provided rather monodisperse QD clusters, 87 ± 4 nm in diameter as analyzed by TEM (Figure 1). Smaller or larger average cluster sizes could be obtained by varying the amount of QDs in the organic phase. The thickness obtained for the silica layer was typically ~ 25 nm (Figure 1), which could be adjusted by changing the amount of TEOS, alcohol or ammonia [17,22,42]. To our knowledge, such

monodisperse and very compact QD clusters entrapped in a silica layer have not yet been reported in literature.

Fluorescence spectroscopy of QD-NSCs showed that the assembly of QDs in clusters and coating with silica did not affect their fluorescence spectrum apart from a very small shift in the emission wavelength (Supporting Information, Figure S2). In order to validate the potential of these silica-coated QD clusters as bright fluorescence probes, the fluorescence signal of individual QD-NSCs was compared to that of single QDs from the same synthesis batch using fluorescence microscopy. Individual QD-NSCs were on average 1500 times brighter than single unmodified QDs. Considering that each QD-NSC presents a 90 nm-QD core and supposing that QDs are well-packed, an estimate of ~ 3700 QDs in each QD-NSCs can be drawn. This strongly suggests that QD-NSCs exhibit a relatively great fluorescence signal despite a limited quenching of the QDs following aggregation, transfer in water and silica growth. The modification of QD optical properties by silica coverage, in particular, was reported by Rogach et al..[28]

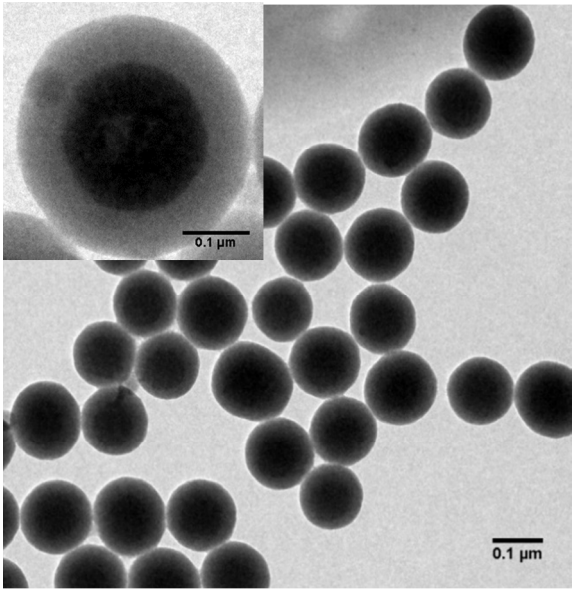

Figure 1: TEM image of silica-coated QD clusters (QD-NSCs). The average size of the clusters presented in this work is of 137 ± 8 nm, which makes them atypically compact as well as monodisperse. Inset: higher magnification of a different sample obtained by slightly increasing the amount of QDs, which resulted in bigger QD-NSCs.

3.2. Synthesis and characterization of P(PC-PTMSi) and P(PC-PTMSi-N_3) copolymers. Bare silica is not adequate for biodetection applications due to strong nonspecific adsorption. Silica surfaces are therefore usually modified by silane chemistry but these surfaces undergo hydrolysis over time, especially in extremely dilute conditions. We reasoned that including multiple anchoring silane groups in a single polymer chain would increase the stability of the organic surface coating compared to molecular mono-silane groups. To this end, we synthesized a multidentate statistical copolymer, P(PC-PTMSi), composed of PTMSi to anchor the polymer on the silica surface and PC to enhance colloidal stability in saline solutions, limit nonspecific adsorption of proteins thanks to the excellent antifouling effect of PC zwitterionic chains, in a 20:80 PTMSi-PC monomer ratio [40,41].

Cyclooctyne-azide click chemistry is a popular and versatile bio-orthogonal conjugation scheme. In order to enable subsequent biomolecular coupling, we therefore chose to incorporate azido-terminated monomers in ~10 % proportion in addition to the zwitterionic and silane monomers to produce the P(PC-PTMSi-N_3) copolymer.

Both polymer syntheses yielded monomer conversion greater than 92%, as determined by ^{1}H-NMR. GPC analysis yielded -average molecular weights (M_n) of 90 kDa with a polydispersity index of 2.5 for P(PC-PTMSi-N_3). ^{1}H NMR and IR spectra of purified polymers confirmed the

presence of both silane and phosphorylcholine units (Supporting Information, Figures S6 and S7), even though FT-IR spectroscopy doesn't show the $-N_3$ moiety. Assuming that the composition of the final polymer is similar to the composition of the initial monomer solution, we calculated an estimate of ~ 50 silanes per polymer chain; this should considerably increase the stability of the outer silica surface chemistry.

3.3. Polymer-capped silica beads preparation. Silica and QD-NSCs were coated with both copolymers by incubation in methanol at 60°C for 2 hours. Water traces were present in the reaction medium since the solvent was not anhydrous and water-mediated Stöber-like protocols were used to synthesize silica beads and QD-NSCs' silica shells. This ensures efficient condensation of the polymer silane groups on the surface of the silica beads [36,46,47]. Following purification, TGA results indicated that P(PC-PTMSi) and P(PC-PTMSi-N_3) effectively coat silica beads with a substantial coverage density of ~ 3 mg of polymer per m^2 silica. The results for P(PC-PTMSi) are presented in Supporting Information (Supporting Information, Figure S8). No substantial differences in surface coverage were revealed for these two copolymers.

3.3.1 Colloidal stability and low-fouling properties. We compared the colloidal stability of P(PC-PTMSi)-coated silica beads with that of bare silica beads in acetate, HEPES/NaCl and bicarbonate buffer. Dynamic light scattering measurements (Supporting Information, Figure S9) showed that bare silica beads and P(PC-PTMSi)-coated silica beads exhibited a narrow-sized monomodal distribution around a 101 nm +/- 10 nm mean hydrodynamic radius value independently from the buffer. Measurements performed one week later on the same samples showed no change in the colloidal stability. Zwitterionic polymers are indeed known to provide high colloidal stability, even under extreme saline conditions. [9,47,48] Zeta potential measurements

gave, for bare silica beads, an average value of – 37.50 mV in acetate buffer pH 4.5, - 20,46 mV in HEPES/NaCl buffer pH 7.4 and – 41.9 mV in bicarbonate buffer pH 9.5. The smaller potential in HEPES/NaCl can be explained by the charge screening in highly saline buffers. Once the silica beads are coated with P(PC-PTMSi), however, they exhibit much reduced zeta potentials, ranging from -11 mV to -5 mV independently from the buffer nature and pH. We attribute this low zeta potential to the neutral overall charge of phosphorylcholine, compared to the negatively charged silanol groups of bare silica. Residual negative zeta potentials may originate from different associated counterions and/or free, non surface-bound silane moieties. Altogether, these results confirm that we effectively succeeded in coating the silica beads with the polymer.

We then tested the antifouling properties of the copolymer coating by comparing protein adsorption on P(PC-PTMSi)-coated silica beads with that on bare silica beads, silica beads coated with a zwitterionic monosilane, the 3(dimethyl-(3-(trimethoxysilyl)propyl)ammonio)propane-1-sulfonate (SBS). Dye-labeled BSA was used as a model protein. After a 30 min incubation of the beads in a concentrated RITC-labeled BSA solution (25 μM) and posterior removal of the unbound proteins by two rounds of centrifugation, the degree of nonspecific adsorption was probed by absorbance measurements at 555 nm (RITC). As shown in Figure 2, the peak absorbance value for bare silica beads is 8.5 times higher than that of P(PC-PTMSi)-coated silica beads. This means that there are 8.5 times more proteins adsorbed on the surface of bare silica than on the silica surface coated with the copolymer. This difference is due to the low fouling properties conferred by the zwitterionic phosphorylcholine moieties to P(PC-PTMSi)-coated silica beads and masking of the negatively charged silica surface.

The low-fouling properties of P(PC-PTMSi) are comparable to those of a sulfobetaine-functionalized monosilane[45].

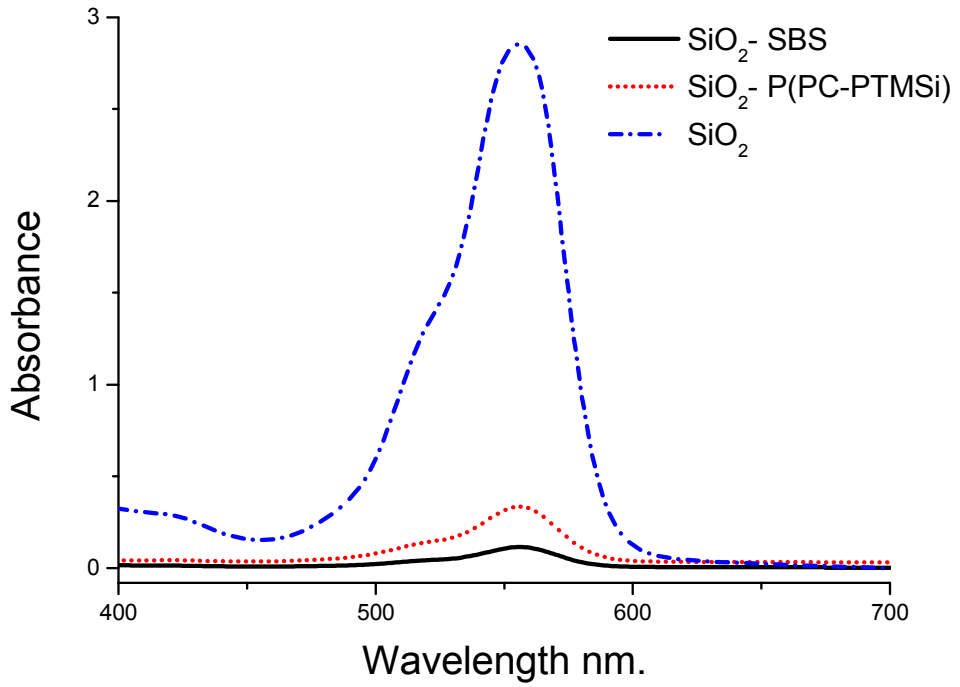

Figure 2: Absorbance values measured for bare silica (SiO_2), P(PC-PTMSi)-coated silica beads (SiO_2- P(PC-PTMSi)) and SBS-coated silica beads (SiO_2- SBS) exposed to RITC-labeled BSA and washed. The characteristic absorbance maximum of RITC, corresponding to the RITC-labeled BSA, can be found at 555nm.

3.3.2 Polymer surface stability. Silica surfaces are usually functionalized using monosilane groups such as those derived from aminopropyltriethoxysilane (APTES) or mercaptopropyltrimethoxysilane (MPTMS) [1,21,46,49]. The covalent Si-O-Si bonds between these molecules and silanol groups on the silica surface are however in constant condensation/hydrolysis equilibrium in aqueous media. Hydrolysis rates can be increased by

varying many parameters like temperature, salinity, particle size or pH [33–36,50]: therefore, its effects can be critical to preserve the beads' low fouling properties and functional moieties.

In this work, we presumed that establishing multiple siloxane bonds would enhance the stability of the polymer on the silica surface. In order to test this hypothesis, the hydrolytic stability of our multidentate polymer was compared to monosilane molecules under three conditions: diluted at physiological pH (0.025 $m^2.mL^{-1}$ at pH 7.4), concentrated at physiological pH (0.2 $m^2.mL^{-1}$ at pH 7.4) and concentrated at slightly basic pH (0.2 $m^2.mL^{-1}$ at pH 8). First, we functionalized silica beads with P(PC-PTMSi-N_3) and labeled them with a Cy3 dye using cyclooctyne-based copper-free click chemistry. Control silica beads coated with a P(PC-PTMSi) copolymer without azido groups showed no labeling. Then, we modified APTES with fluorescein-NHS ester and thereafter proceeded to bind the resulting f-APTES molecule to silica beads. Both, fluorescently-labeled APTES and multidentate polymer samples were left to incubate, in the dark and at room temperature, in the three different conditions mentioned above. At each evaluated time point, a small sample of ~ 0.1 m^2 was taken and centrifuged once to separate free dye-labeled molecules from those bound to the silica beads. Absorbance measurements of resuspended pellets enabled us to estimate the fraction of functionalization molecules still bound to the beads.

The results are displayed on Figure 3. In a physiological pH buffer and in a relatively concentrated solution of beads (0.2 $m^2.mL^{-1}$), about 50% of dye-labeled APTES molecules were detached from the surface after 6 days of incubation. An even more significant and faster loss of APTES-bound dye molecules occurred under slightly basic conditions (pH 8) and led to a 60% loss in 6 days: we effectively observed an increase of hydrolysis with pH, as demonstrated by the pioneering works of Brady et al.[35] Interestingly, incubating dye-APTES labeled silica beads in

neutral pH conditions at lower concentration (0.025 $m^2.mL^{-1}$) led to a rapid loss of APTES-bound dye molecules, suggesting that dilute conditions favor displacement of the equilibrium towards hydrolysis. This loss of surface functionality represents a strong limitation, especially in the context of precise detection applications at the single molecule level, which occur by essence in extremely dilute conditions. In contrast, incubation of dye-labeled P(PC-PTMSi-N_3)-coated silica beads under the three conditions mentioned earlier show that the polymer remain strongly bound to the surface of silica beads after 6 days, even in slightly basic or dilute conditions. This increased stability can be attributed to the multidentate nature of the polymer, which presents many silane groups to bind to the nanoparticle surface.

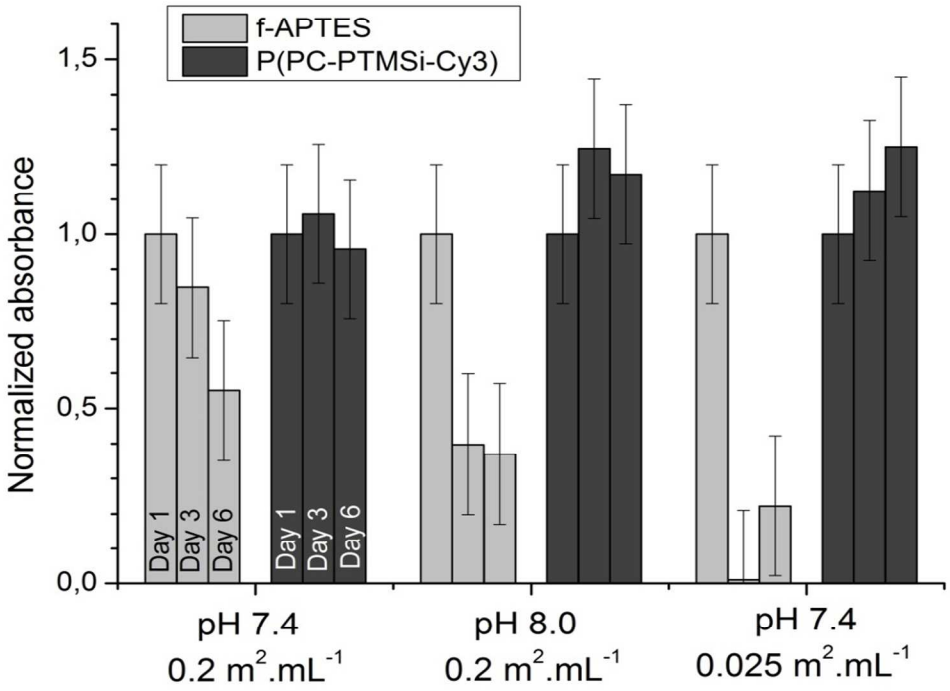

Figure 3: Normalized absorbance values for f-APTES- and P(PC-PTMSi-Cy3)-grafted silica beads at three different pH and concentration conditions. Absorbance values were measured every 3 days at 494 nm (fluorescein) and 570 nm (Cy3) for f-APTES and P(PC-PTMSi-Cy3)

grafted silica beads, respectively. Absorbance values were normalized to 1 at time zero. Error bars were estimated from reproducibility variations, including variations in silica amount after purification, which may account for values slightly above 1 within error bars.

3.4. Bioconjugation of the clusters. Cyclooctyne-azide click chemistry was chosen as a versatile bio-orthogonal conjugation technique. To demonstrate the potential of P(PC-PTMSi-N_3)-coated QD-NSCs for biodetection, we conjugated them to streptavidin and tested them on biotinylated substrates as a model targeting system. To this end, streptavidin was functionalized with DBCO, a strained alkyne moiety which enables cyclooctyne-azide coupling without the need for copper (I) catalyst. An NHS-ester – DBCO linker was randomly reacted with some lysines available on the streptavidin surface and the protein was purified by ultrafiltration. A 3:1 DBCO-NHS:streptavidin molar ratio was chosen to enable functionalization while keeping a low number of DBCO per streptavidin. Indeed, since we aim at creating a versatile platform, this procedure should be envisioned for reactions such as antibody conjugation and overconjugating antibodies can lead to their loss of functionality. P(PC-PTMSi-N_3)-coated QD-NSC beads were then reacted with DBCO-streptavidin and purified by centrifugation without any appreciable loss of colloidal stability. Microscopic examination of biotinylated agarose beads incubated with these streptavidin-QD-NSCs showed a strong fluorescent signal (Figure 4(A)). By contrast, the interactions of the control, P(PC-PTMSi)-coated QD-NSCs, with biotin-bearing agarose surfaces appear as negligible, a fact that can be attributable to the low-fouling properties of the copolymer (Figure 4(B)). Altogether, these results demonstrate that DBCO-streptavidin binds to the P(PC-PTMSi-N_3)-coated QD-NSC specifically via cyclooctyne-azide conjugation and that the anchored streptavidin retains its biotin-recognition functionality.

An additional control consisting of QD-NSCs mixed with non-DBCO streptavidin also showed very little nonspecific fluorescent signal (Supporting Information, Figure S10). When non-DBCO streptavidin is mixed with the P(PC-PTMSi-N_3)-coated QD-NSCs, some residual non-specific binding is observed, as shown above with BSA. Increasing the number of washing cycles after exposure to proteins (streptavidin or BSA in our case) could decrease non-specific binding; an acceptable trade-off between controlling non-specific binding and favoring a less laborious sample preparation process shall then be defined ad-hoc.

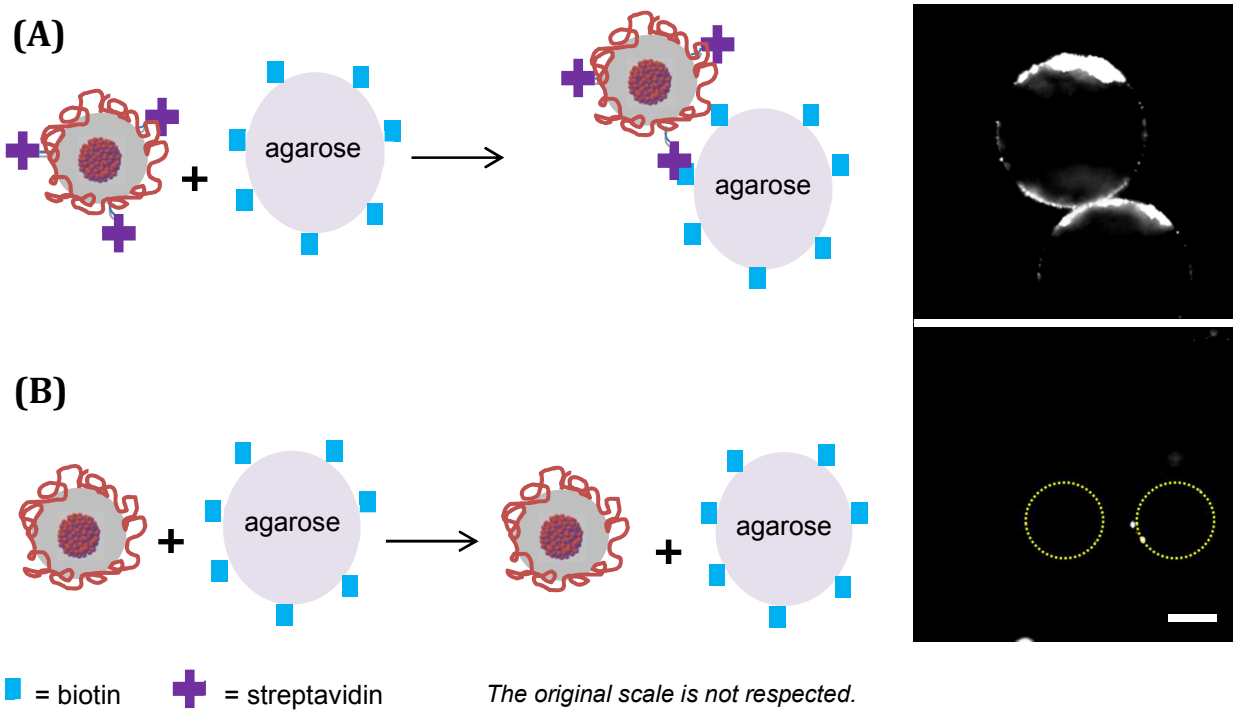

Figure 4: P(PC-TMSi-N_3)-coated QD-NSC beads reacted with streptavidin **(A)** or as such **(B)** were left to react for 15 min with biotin agarose beads in HEPES, 10 mM, 150 mM, pH 7.4 and washed thereafter. The epifluorescence microscopy pictures on the right correspond to biotin agarose beads from both experiments, respectively, deposited onto a coverslip. The yellow dotted circle on the bottom picture delimitates the agarose beads, which cannot be seen by

fluorescence. Scale bar= 10 μm

4. CONCLUSION

In this work, we presented a multi-step strategy to design colloidal fluorescent nanosized clusters (NSCs) based on silica-embedded quantum dots (QDs). Firstly, QD clusters were formed in a cetyltrimethylammonium bromide-mediated microemulsion and a silica shell was subsequently grown on their surface by a Stöber-inspired process. This reproducible methodology led to compact and very bright clusters of approximately 130 nm diameter.

A particular focus was made on the surface chemistry tailoring of QD-NSCs with the synthesis and characterization of an original multidentate polymer-silane hybrid. After this polymer-silane hybrid was grafted on the surface of Stöber silica beads, we demonstrated that its zwitterionic chain was indeed responsible for a low-fouling effect with regards to a protein such as bovine serum albumine and for the colloidal stability of copolymer-capped silica beads in a physiological buffer. Moreover, the multiple silane anchoring functions of the polymer-silane hybrid seemed to contribute to its better anchoring on the surface of silica beads when compared to individual silane chains, which were more prone to unbinding over time due to hydrolysis.

After the polymer-silane hybrid was grafted onto the silica shell of the QD-NSCs, its azide moiety was effectively reacted with a cyclooctyne-functionalized protein as demonstrated by a specific biomolecular affinity test.

The nanobeads that have been designed constitute a versatile biosensing tool that can be tailored beyond the proof-of-concept showed in this paper e.g. by changing the nature of the inorganic particles encapsulated or the chemical functions available on the surface. Taken

altogether, the results obtained provide interesting perspectives in terms of applications, for example as ultrasensitive single-molecule detection probes within complex biological samples or as signal amplifiers in rare target detection.

ASSOCIATED CONTENT

Synthesis and size characterization of bare silica beads, synthesis of QDs, photoluminescence spectrum for QDs and QDs-NSCs, synthesis and characterization of the *N*-(11-azido-3,6,9-trioxaundecan)methacrylamide (IR Spectroscopy, ^{1}H NMR and ^{13}C NMR in $CDCl_3$), reaction scheme for the synthesis of P(PC-PTMSi-N_3), additional characterization of P(PC-PTMSi-N_3) (IR Spectroscopy, ^{1}H NMR), TGA results, intensity-weighted size distribution obtained from dynamic light scattering at one angle for P(PC-PTMSi)-coated silica beads in HEPES/NaCl buffer, additional control experiment to the bioconjugation experiment with STA without a dibenzocyclooctyne moieity. (PDF)

AUTHOR INFORMATION

Corresponding Author

*E-mail: thomas.pons@espci.fr

Present Addresses

† UMR 8638 CNRS, Faculté de Pharmacie de Paris, Université Paris Descartes, Sorbonne Paris Cité, 4 avenue de l'observatoire, 75006 Paris, France.

Author Contributions

The manuscript was written through contributions of all authors. All authors have given approval to the final version of the manuscript.

Funding Sources

L.T.A. acknowledges funding from PSL Research University.

ACKNOWLEDGMENT

The authors thank the LCO Laboratory (ESPCI, Paris, France) and especially Thomas Aubineau for providing the ^{1}H NMR measurements as well as the SIMM laboratories (ESPCI, Paris, France) for the sharing of their equipment.

REFERENCES

(1) Jun, B. H.; Hwang, D. W.; Jung, H. S.; Jang, J.; Kim, H.; Kang, H.; Kang, T.; Kyeong, S.; Lee, H.; Jeong, D. H.; Kang, K. W.; Youn, H.; Lee, D. S.; Lee, Y. S. Ultrasensitive, Biocompatible, Quantum-Dot-Embedded Silica Nanoparticles for Bioimaging. *Adv. Funct. Mater.* **2012**, *22* (9), 1843–1849.

(2) Li, X.; Li, W.; Yang, Q.; Gong, X.; Guo, W.; Dong, C.; Liu, J.; Xuan, L.; Chang, J. Rapid and Quantitative Detection of Prostate Specific Antigen with a Quantum Dot Nanobeads-Based Immunochromatography Test Strip. *ACS Appl. Mater. Interfaces* **2014**, *6* (9), 6406–6414.

(3) Esteve-Turrillas, F. A.; Abad-Fuentes, A. Applications of Quantum Dots as Probes in Immunosensing of Small-Sized Analytes. *Biosens. Bioelectron.* **2013**, *41*, 12–29.

(4) Sapsford, K. E.; Pons, T.; Medintz, I. L.; Mattoussi, H. Biosensing with Luminescent Semiconductor Quantum Dots. *Sensors* **2006**, *6* (8), 925–953.

(5) Bruchez Jr., M.; Moronne, M.; Gin, P.; Weiss, S.; Alivisatos, A. P. Semiconductor Nanocrystals as Fluorescent Biological Labels. *Science* **1998**, *281* (5385), 2013–2016.

(6) Xing, Y.; Chaudry, Q.; Shen, C.; Kong, K. Y.; Zhau, H. E.; Chung, L. W.; Petros, J. a; O'Regan, R. M.; Yezhelyev, M. V; Simons, J. W.; Wang, M. D.; Nie, S. Bioconjugated Quantum Dots for Multiplexed and Quantitative Immunohistochemistry. *Nat. Protoc.* **2007**, *2* (5), 1152–1165.

(7) Speranskaya, E. S.; Beloglazova, N. V; Lenain, P.; De Saeger, S.; Wang, Z.; Zhang, S.; Hens, Z.; Knopp, D.; Niessner, R.; Potapkin, D. V; Goryacheva, I. Y. Polymer-Coated Fluorescent CdSe-Based Quantum Dots for Application in Immunoassay. *Biosens. Bioelectron.* **2014**, *53*, 225–231.

(8) Hu, S. H.; Gao, X. Stable Encapsulation of Quantum Dot Barcodes with Silica Shells. *Adv. Funct. Mater.* **2010**, *20* (21), 3721–3726.

(9) Giovanelli, E.; Muro, E.; Sitbon, G.; Hanafi, M.; Pons, T.; Dubertret, B.; Lequeux, N. Highly Enhanced Affinity of Multidentate versus Bidentate Zwitterionic Ligands for Long-Term Quantum Dot Bioimaging. *Langmuir* **2012**, *28* (43), 15177–15184.

(10) Tasso, M.; Giovanelli, E.; Zala, D.; Bouccara, S.; Fragola, A.; Hanafi, M.; Lenkei, Z.; Pons, T.; Lequeux, N. Sulfobetaine-Vinylimidazole Block Copolymers: A Robust Quantum Dot Surface Chemistry Expanding Bioimaging's Horizons. *ACS Nano* **2015**, *9* (11), 11479–11489.

(11) Zhang, Y.; Clapp, A. Overview of Stabilizing Ligands for Biocompatible Quantum Dot Nanocrystals. *Sensors (Basel).* **2011**, *11* (12), 11036–11055.

(12) Marotta, R.; Manna, L.; Pellegrino, T.; Corato, D. I.; Al, E. T. Multifunctional Nanobeads Based on Quantum Dots and Magnetic Cell Targeting and Sorting. *ACS Nano* **2011**, *5* (2), 1109–1121.

(13) Yu, W. W.; Chang, E.; Falkner, J. C.; Zhang, J.; Al-Somali, A. M.; Sayes, C. M.; Johns, J.; Drezek, R.; Colvin, V. L. Forming Biocompatible and Nonaggregated Nanocrystals in Water Using Amphiphilic Polymers. *J. Am. Chem. Soc.* **2007**, *129* (10), 2871–2879.

(14) Pellegrino, T.; Manna, L.; Kudera, S.; Liedl, T.; Koktysh, D.; Rogach, A. L.; Keller, S.; Rädler, J.; Natile, G.; Parak, W. J. Hydrophobic Nanocrystals Coated with an Amphiphilic Polymer Shell: A General Route to Water Soluble Nanocrystals. *Nano Lett.* **2004**, *4* (4), 703–707.

(15) Palui, G.; Aldeek, F.; Wang, W.; Mattoussi, H. Strategies for Interfacing Inorganic Nanocrystals with Biological Systems Based on Polymer-Coating. *Chem. Soc. Rev.* **2014**, *44*, 193–227.

(16) Pietra, F.; van Dijk - Moes, R. J. A.; Ke, X.; Bals, S.; Van Tendeloo, G.; de Mello Donega, C.; Vanmaekelbergh, D. Synthesis of Highly Luminescent Silica-Coated CdSe/CdS Nanorods. *Chem. Mater.* **2013**, *25* (17), 3427–3434.

(17) Darbandi, M.; Thomann, R.; Nann, T. Single Quantum Dots in Silica Spheres by Microemulsion Synthesis. *Chem. Mater.* **2005**, *17* (23), 5720–5725.

(18) Foda, M. F.; Huang, L.; Shao, F.; Han, H.-Y. Biocompatible and Highly Luminescent Near-Infrared CuInS2/ZnS Quantum Dots Embedded Silica Beads for Cancer Cell Imaging. *ACS Appl. Mater. Interfaces* **2014**, *6* (3), 2011–2017.

(19) Gerion, D.; Pinaud, F.; Williams, S. C.; Parak, W. J.; Zanchet, D.; Weiss, S.; Alivisatos, A. P. Synthesis and Properties of Biocompatible Water-Soluble Silica-Coated CdSe / ZnS Semiconductor Quantum Dots. *J. Phys. Chem. B* **2001**, *105*, 8861–8871.

(20) Qiu, P.; Jensen, C.; Charity, N.; Towner, R.; Mao, C. Oil Phase Evaporation-Induced Self-Assembly of Hydrophobic Nanoparticles into Spherical Clusters with Controlled Surface Chemistry in an Oil-in-Water Dispersion and Comparison of Behaviors of Individual and Clustered Iron Oxide Nanoparticles. *J. Am. Chem. Soc.* **2010**, *132* (50), 17724–17732.

(21) Liberman, A.; Mendez, N.; Trogler, W. C.; Kummel, A. C. Synthesis and Surface Functionalization of Silica Nanoparticles for Nanomedicine. *Surf. Sci. Rep.* **2014**, *69* (2–3), 132–158.

(22) Nallathamby, P. D.; Hopf, J.; Irimata, L. E.; McGinnity, T. L.; Roeder, R. K. Preparation of Fluorescent Au–SiO2 Core–shell Nanoparticles and Nanorods with Tunable Silica Shell Thickness and Surface Modification for Immunotargeting. *J. Mater. Chem. B* **2016**, *4* (32), 5418–5428.

(23) Hu, X.; Gao, X. Silica-Polymer Dual Layer-Encapsulated Quantum Dots with Remarkable Stability. *ACS Nano* **2010**, *4* (10), 6080–6086.

(24) D'Amico, M.; Fiorica, C.; Palumbo, F. S.; Militello, V.; Leone, M.; Dubertret, B.; Pitarresi, G.; Giammona, G. Uptake of Silica Covered Quantum Dots into Living Cells: Long Term Vitality and Morphology Study on Hyaluronic Acid Biomaterials. *Mater. Sci. Eng. C* **2016**, *67*, 231–236.

(25) Yi, D. K.; Selvan, S. T.; Lee, S. S.; Papaefthymiou, G. C.; Kundaliya, D.; Ying, J. Y. Silica-Coated Nanocomposites of Magnetic Nanoparticles and Quantum Dots. *J. Am. Chem. Soc.* **2005**, *127* (14), 4990–4991.

(26) Chan, Y.; Zimmer, J. P.; Stroh, M.; Steckel, J. S.; Jain, R. K.; Bawendi, M. G. Incorporation of Luminescent Nanocrystals into Monodisperse Core-Shell Silica Microspheres. *Adv. Mater.* **2004**, *16* (23–24), 2092–2097.

(27) Dubois, F.; Mahler, B.; Dubertret, B.; Doris, E.; Mioskowski, C. A Versatile Strategy for Quantum Dot Ligand Exchange. *J. Am. Chem. Soc.* **2007**, *129* (3), 482–483.

(28) Rogach, A. L.; Nagesha, D.; Ostrander, J. W.; Giersig, M.; Kotov, N. A. "Raisin Bun"-type Composite Spheres of Silica and Semiconductor Nanocrystals. *Chem. Mater.* **2000**, *12* (9), 2676–2685.

(29) Han, M.; Gao, X.; Su, J. Z.; Nie, S. Quantum-Dot-Tagged Microbeads for Multiplexed Optical Coding of Biomolecules. *Nat. Biotechnol.* **2001**, *19* (7), 631–635.

(30) Wang, J.; Li, W.; Zhu, J. Encapsulation of Inorganic Nanoparticles into Block Copolymer Micellar Aggregates: Strategies and Precise Localization of Nanoparticles. *Polymer* **2014**, *55* (5), 1079–1096.

(31) Bai, F.; Wang, D.; Huo, Z.; Chen, W.; Liu, L.; Liang, X.; Chen, C.; Wang, X.; Peng, Q.; Li, Y. A Versatile Bottom-up Assembly Approach to Colloidal Spheres from Nanocrystals. *Angew. Chem. Int. Ed. Engl.* **2007**, *46* (35), 6650–6653.

(32) Farmer, S. C.; Patten, T. E. Photoluminescent Polymer/Quantum Dot Composite Nanoparticles. *Chem. Mater.* **2001**, *13* (11), 3920–3926.

(33) Diedrich, T.; Dybowska, A.; Schott, J.; Valsami-Jones, E.; Oelkers, E. H. The Dissolution Rates of SiO 2 Nanoparticles As a Function of Particle Size. *Environ. Sci. Technol.* **2012**, *46* (9), 4909–4915.

(34) Mahon, E.; Hristov, D. R.; Dawson, K. A. Stabilising Fluorescent Silica Nanoparticles against Dissolution Effects for Biological Studies. *Chem. Commun.* **2012**, *48* (64), 7970–7972.

(35) Brady, P. V.; Walther, J. V. Controls on Silicate Dissolution Rates in Neutral and Basic pH Solutions at 25°C. *Geochim. Cosmochim. Acta* **1989**, *53* (11), 2823–2830.

(36) Smith, E. A.; Chen, W. How to Prevent the Loss of Surface Functionality Derived from Aminosilanes. *Langmuir* **2008**, *24* (21), 12405–12409.

(37) Ma, L.; Tu, C.; Le, P.; Chitoor, S.; Lim, S. J.; Zahid, M. U.; Teng, K. W.; Ge, P.; Selvin, P. R.; Smith, A. M. Multidentate Polymer Coatings for Compact and Homogeneous Quantum Dots with Efficient Bioconjugation. *J. Am. Chem. Soc.* **2016**, *138* (10), 3382–3394.

(38) Yuan, B.; Chen, Q.; Ding, W. Q.; Liu, P. S.; Wu, S. S.; Lin, S. C.; Shen, J.; Gai, Y. Copolymer Coatings Consisting of 2-Methacryloyloxyethyl Phosphorylcholine and 3-Methacryloxypropyl Trimethoxysilane via ATRP to Improve Cellulose Biocompatibility. *ACS Appl. Mater. Interfaces* **2012**, *4* (8), 4031–4039.

(39) Ishihara, K.; Nomura, H.; Mihara, T.; Kurita, K.; Iwasaki, Y.; Nakabayashi, N. Why Do Phospholipid Polymers Reduce Protein Adsorption? *J. Biomed. Mater. Res.* **1998**, *39* (2), 323–330.

(40) Schlenoff, J. B. Zwitteration: Coating Surfaces with Zwitterionic Functionality to Reduce Nonspecific Adsorption. *Langmuir* **2014**, *30* (32), 9625–9636.

(41) Chen, S.; Li, L.; Zhao, C.; Zheng, J. Surface Hydration: Principles and Applications toward Low-Fouling/nonfouling Biomaterials. *Polymer* **2010**, *51* (23), 5283–5293.

(42) Stöber, W.; Fink, A.; Bohn, E. Controlled Growth of Monodisperse Silica Spheres in the Micron Size Range. *J. Colloid Interface Sci.* **1968**, *26* (1), 62–69.

(43) Bernardin, A.; Cazet, A.; Guyon, L.; Delannoy, P.; Vinet, F.; Bonnaffé, D.; Texier, I. Copper-Free Click Chemistry for Highly Luminescent Quantum Dot Conjugates: Application to *in Vivo* Metabolic Imaging. *Bioconjugate Chem.* **2010**, *21* (4), 583–588.

(44) Diamandis, E. P.; Christopoulos, T. K. The Biotin-(Strept)avidin System: Principles and Applications in Biotechnology. *Clin. Chem.* **1991**, *37* (5), 625–636.

(45) Estephan, Z. G.; Jaber, J. a.; Schlenoff, J. B. Zwitterion-Stabilized Silica Nanoparticles: Toward Nonstick Nano. *Langmuir* **2010**, *26* (22), 16884–16889.

(46) Howarter, J. A.; Youngblood, J. P. Optimization of Silica Silanization by 3-Aminopropyltriethoxysilane. *Langmuir* **2006**, *22* (26), 11142–11147.

(47) Yu, Y. Y.; Chen, C. Y.; Chen, W. C. Synthesis and Characterization of Organic-Inorganic Hybrid Thin Films from Poly(acrylic) and Monodispersed Colloidal Silica. *Polymer* **2002**, *44* (3), 593–601.

(48) Zou, H.; Wu, S.; Shen, J. Polymer / Silica Nanocomposites : Preparation , Characterization , Properties , and. *Chem. Rev.* **2008**, *108*, 3893–3957.

(49) Lin, G. G.; Scott, J. G. How to Prepare Reproducible, Homogeneous, and Hydrolytically Stable Aminosilane-Derived Layers on Silica. *Langmuir* **2012**, *100* (2), 130–134.

(50) Icenhower, J. P.; Dove, P. M. The Dissolution Kinetics of Amorphous Silica into Sodium Chloride Solutions: Effects of Temperature and Ionic Strength. *Geochim. Cosmochim. Acta* **2000**, *64* (24), 4193–4203.

TOC GRAPHIC